Molecular Cancer Therapeutics

T-Type Ca^{2+} Channel Inhibition Sensitizes Ovarian Cancer to Carboplatin

Barbara Dziegielewska[1], Eli V. Casarez[2], Wesley Z. Yang[1], Lloyd S. Gray[3], Jaroslaw Dziegielewski[1,4], and Jill K. Slack-Davis[2,4]

Abstract

Ovarian cancer is the deadliest gynecologic cancer, due in large part to the diagnosis of advanced stage disease, the development of platinum resistance, and inadequate treatment alternatives. Recent studies by our group and others have shown that T-type calcium (Ca^{2+}) channels play a reinforcing role in cancer cell proliferation, cell-cycle progression, and apoptosis evasion. Therefore, we investigated whether T-type Ca^{2+} channels affect ovarian tumor growth and response to platinum agents. Inhibition of T-type Ca^{2+} channels with mibefradil or by silencing expression resulted in growth suppression in ovarian cancer cells with a simultaneous increase in apoptosis, which was accompanied by decreased expression of the antiapoptotic gene survivin (*BIRC5*). Analysis of intracellular signaling revealed mibefradil reduced AKT phosphorylation, increased the levels and nuclear retention of FOXO transcription factors that repress *BIRC5* expression, and decreased the expression of FOXM1, which promotes *BIRC5* expression. Combining carboplatin with mibefradil synergistically increased apoptosis *in vitro*. Importantly, mibefradil rendered platinum-resistant ovarian tumors sensitive to carboplatin in a mouse model of peritoneal metastasis. Together, the data provide rationale for future use of T-type channel antagonists together with platinum agents for the treatment of ovarian cancer. *Mol Cancer Ther; 15(3); 460–70. ©2016 AACR.*

Introduction

Ovarian cancer is the deadliest gynecologic malignancy and the fifth leading cause of all cancer-related death in women. According to Surveillance Epidemiology and End Results estimates, approximately 22,000 women in the United States will be diagnosed with ovarian cancer, and more than 14,000 patients will die of this disease (1). More than 75% of the incident cases are detected after metastatic spread (Stages III and IV), where the survival rate at five years is only 10% to 20%. Standard treatment consists of surgical cytoreduction and cytotoxic chemotherapy. Although a majority of advanced stage patients achieve a complete response to standard platinum/taxane–based chemotherapy, as many as 80% recur within 2 years and will eventually succumb to platinum-resistant disease. Despite advances in cytotoxic therapy, resistance to platinum agents remains a significant hurdle to overcome.

Calcium (Ca^{2+}) is a crucial second messenger in all eukaryotic cells (2). The relationship between Ca^{2+} signaling and cardiovascular or neurologic diseases has been studied for decades. Indeed, classes of drugs targeting particular Ca^{2+} channels are used to treat hypertension, angina, and other cardiovascular conditions. More recently, the contribution of overexpression and/or aberrant activation of Ca^{2+}-specific channels and Ca^{2+}-regulated intracellular pathways to cancer progression has been reported (3). Voltage-activated Ca^{2+} channels provide a pathway for rapid influx of Ca^{2+} into cells. Among them, the low voltage–activated Ca^{2+} channel family (Cav3, commonly called T-type Ca^{2+} channels) is functionally linked to many physiologic processes (4) and is aberrantly expressed in cancer, including ovarian tumors and cell lines (5, 6). Recent data demonstrate that the inhibition of T-type Ca^{2+} channels in ovarian cancer cells disturbs cell-cycle progression, decreases proliferation, and enhances cell death (5, 6). However, the detailed molecular mechanisms of this inhibition are still unknown. We previously reported that T-type Ca^{2+} channel blockers, specifically mibefradil, induce apoptosis in glioblastoma and colon cancer cells by the suppression of the PI3K/AKT pathway (7) and the activation of p53 and the p38/MAPK pathway (8), respectively. Upon T-type Ca^{2+} channel inhibition, apoptosis is manifested as changes in expression of several pro and antiapoptotic proteins (7, 8), including the antiapoptotic protein survivin.

Survivin (encoded by *BIRC5*) is one of the antiapoptotic proteins belonging to the inhibitor of apoptosis (IAP) family (9). It is important for the inhibition of apoptosis and essential in the regulation of mitosis (10), autophagy (11), and DNA damage repair (12). Survivin is overexpressed in many cancers, including ovarian (13–17), and as such could serve as both molecular target and biomarker for response to therapy and patient survival (18, 19). Several mechanisms regulating survivin gene expression

[1]Department of Radiation Oncology, University of Virginia, Charlottesville, Virginia. [2]Department of Microbiology, Immunology and Cancer Biology, University of Virginia, Charlottesville, Virginia. [3]Cavion LLC, Charlottesville, Virginia. [4]Cancer Center, University of Virginia, Charlottesville, Virginia.

Note: Supplementary data for this article are available at Molecular Cancer Therapeutics Online (http://mct.aacrjournals.org/).

Prior presentation: Preliminary account of this study was presented at the AACR Annual Meetings 2013 and 2015.

Corresponding Author: Jill K. Slack-Davis, University of Virginia, PO Box 800734, 345 Crispell Drive, MR-6, B709, Charlottesville, VA 22908. Phone: 434-243-8579; Fax: 434-243-7244; E-mail: jks6a@virginia.edu

doi: 10.1158/1535-7163.MCT-15-0456

and activity in cancer cells have been reported, including transcriptional regulation (20), posttranslational modification such as phosphorylation, acetylation and ubiquitination (21), and shuttling between the nucleus and cytoplasm (22). However, nonmalignant cells also use those pathways to control normal physiologic functions of survivin. Therefore, we postulate that inhibiting survivin expression by blocking upstream pathways that are deregulated in cancer would allow for more specific targeting of survivin in cancer versus normal tissues. One such pathway involves PI3K/AKT regulation of forkhead box transcription factors acting either as activators (FOXM1; refs. 23, 24) or repressors (FOXO1/FOXO3A; refs. 25, 26) of *BIRC5* expression.

Abnormal expression of antiapoptotic proteins is commonly observed in ovarian tumors and associated with their aggressiveness and resistance to cytotoxic therapy (16, 27). Therefore, intervention in cell death pathways is considered an effective approach to increase cancer response to therapy (18, 28). Here, we investigated the contribution of T-type Ca^{2+} channels to ovarian cancer cell growth and tumor progression. We report that the loss of expression or inhibition of T-type Ca^{2+} channels with mibefradil induced apoptosis in cultured ovarian cancer cell lines. Apoptosis was accompanied by decreased AKT phosphorylation and alterations in FOXO and FOXM1 expression, culminating in reduced survivin expression. Importantly, pretreatment of platinum-resistant ovarian cancer cells with mibefradil rendered them sensitive to carboplatin *in vitro* and significantly hindered tumor growth *in vivo*. Together, our data support the rationale for using T-type Ca^{2+} channel blockers in the treatment of platinum-resistant ovarian cancer.

Materials and Methods

Cell culture and drug treatment

Human ovarian cancer cell lines were purchased from ATCC or Sigma-Aldrich; SKOV3.ip1 were generously provided by Dr. Anil Sood (MD Anderson Cancer Center, Houston, TX). They were maintained in a 37°C/5% CO_2-humidified chamber in RPMI1640 supplemented with 10% FBS (A2780 and A2780Cis) or with sodium bicarbonate, sodium pyruvate, and 10% FBS (IGROV-1) or McCoy supplemented with 15% FBS (SKOV3.ip1). A2780Cis cells were cultured in 1 μmol/L cisplatin every third passage. None of the lines have been tested or authenticated. All cell culture materials and supplies were from Life Technologies Gibco. Mibefradil, a generous gift from Cavion LLC, was suspended in DMSO; cisplatin (Sigma-Aldrich) was suspended in sterile water. Carboplatin was obtained from the University of Virginia Pharmacy (Charlottesville, VA) as a 10 mg/mL stock solution in PBS. Cells were treated with the indicated concentrations of antagonists or platinum agents at 37°C for times indicated as single agents (see Figure legends). Drug combination studies were performed by treating cells for 24 hours with the indicated concentrations of mibefradil and then replacing the mibefradil-containing media with media containing the indicated concentrations of carboplatin or vehicle for another 24 to 72 hours.

siRNA transfection

Cells were transfected with 25 nmol/L of siRNA targeted against *CACNA1G* or *CACNA1H* T-type channel subunits (Supplementary Table S1), or nontargeted scrambled control siRNA, using Lipofectamine RNAiMax (Life Technologies) as described previously (8). After 72 hours, cells were harvested and processed for total RNA isolation or subjected to proliferation, cell death, or Western blot assays.

qRT-PCR for gene expression

Total RNA was isolated using Mini Plus RNeasy Kit (Qiagen), and 1 μg was used for cDNA synthesis using iScript cDNA Synthesis Kit (Bio-Rad Laboratories). Each qPCR reaction was done in triplicate using SsoFast EvaGreen Supermix (Bio-Rad), including 50 ng of cDNA as a template and 0.5 μmol/L of specific primers (Supplementary Table S2; refs. 8, 29). Conditions for amplification were as follows: initial denaturation 98°C for 30 seconds, then 40 cycles of denaturation for 5 seconds at 98°C and annealing with extension for 5 seconds at 62°C. Relative gene expression of specific genes of T-type Ca^{2+} channels or *BIRC5* was normalized to *GAPDH*, β-glucouronidase (*GUSB*), or *ACTB* expression and calculated by the formula $2^{-\Delta\Delta C}{}_t$ by subtracting the C_t value of *GAPDH*, *GUSB*, or *ACTB* and then the C_t value of untreated control (30).

Cell viability, metabolic activity, and proliferation

The viability of treated cells was assessed using trypan blue exclusion. Following treatment cells were collected by trypsinization, stained with trypan blue (0.04%) for 10 minutes, and the total cells and percentage of nonviable cells were counted using Automated Cell Counter (Bio-Rad). Proliferation/Viability was determined by AlamarBlue (Life Technologies) after 72-hour drug treatment. The proliferation rate was assessed by staining cells treated with indicated drugs or vehicle control for 72 hours with Sulforhodamine B (SRB; Sigma-Aldrich) or using the CyQUANT assay following the manufacturer's instructions (Life Technologies). For drug combination studies, cells were treated first with mibefradil for 24 hours. Mibefradil-containing media were then replaced with either fresh media or media containing carboplatin, and the cells were incubated continuously at 37°C for additional 24 hours. For A2780Cis and IGROV-1 cells, the results for mibefradil-induced drug synergy with carboplatin from CyQUANT proliferation assay were confirmed with longer time incubation with carboplatin (72 hours) in SRB assay.

Cell-cycle distribution

Cells were allowed to attach/recover overnight and treated with studied agents (or sham-treated) for 0 to 24 hours. Bromodeoxyuridine (BrdUrd, BD Pharmingen) was added for the last hour of drug incubation to a final concentration of 10 μmol/L. Samples were collected (including floating cells) and processed using BD Pharmingen BrdU Flow Kit according to the instruction manual. Two-dimensional (BrdUrd-FITC vs. 7-AAD) flow cytometry analyses were performed on a FACSCalibur instrument, quantified using CellQuest software, and analyzed using FlowJo or ModFit Software (Flow Cytometry Core, University of Virginia, Charlottesville, VA).

Apoptosis

Mechanism of cell death induced by mibefradil, carboplatin, or the combination of both was evaluated by Annexin V-FITC/Propidium Iodide (PI) staining (BD Biosciences). Briefly, the cells were plated for 24 hours, treated with mibefradil (6 μmol/L) alone and/or in combination with increasing concentrations of carboplatin (1–10 μg/mL), collected, washed with PBS, and stained with Annexin V-FITC and PI for 15 minutes at room

temperature according to the manufacturer's suggestions (BD Pharmingen). Live cells were analyzed within one hour by 2D flow cytometry (Flow Cytometry Core, University of Virginia, Charlottesville, VA).

Western blotting

Following different incubation times with the drug, the cells were collected, washed with ice-cold PBS, and lysed in modified RIPA buffer (Tris HCl 50 mmol/L, NaCl 150 mmol/L, glycerol 10%, EDTA 5 mmol/L, EGTA 5 mmol/L, Triton X-100 0.5%, deoxycholate 0.5%, CHAPS 0.5%, and protease/phosphatase inhibitors). To assess intracellular distribution of proteins, the cells were processed with NE-PER Reagents (Pierce/Thermo Scientific) to separate nuclear and cytosolic proteins. Equal amounts of protein were resolved on 4% to 20% gradient gels (TGX Criterion, Bio-Rad), transferred to nitrocellulose, and probed with specific antibodies against Rb phospho-Ser780 (Cell Signaling Technology, CST #9307), Rb (CST #9309), cyclin D1 (CST #2926), survivin (CST #2808), PARP (Santa Cruz Biotechnology, SCB sc-8007), cleaved caspase-9 (CST #9505), cleaved caspase-7 (CST #8438), AKT phospho-Ser473 (CST #4051), AKT phospho-Thr308 (CST #2965), AKT (CST #9272), FOXM1 (CST #5436), FOXO1 (CST #2880), FOXO3A (CST #2497), lamin A/C (SCB sc-7292), β-actin (Sigma A5316), and α-tubulin (Sigma T6074). Quantification of signal intensity was performed using a Two-Color Li-COR Odyssey Imager and Software (Li-COR Biosciences).

Chromatin immunoprecipitation

Chromatin immunoprecipitation (ChIP) was performed according to the published protocol (31). Briefly, cells were treated with 10 μmol/L mibefradil (or 0.1% DMSO) for 24 hours. Protein–DNA macromolecules were cross-linked with 1% formaldehyde for 10 minutes at room temperature. Cells were washed and scraped in PBS, collected by centrifugation at 1,000 × *g* for 10 minutes at 4°C, resuspended in lysis buffer containing 1% SDS, protease inhibitors (Pierce), and sonicated using Branson Sonifier 400 W Cell Disruptor to 200–1,000 bp DNA size fractions. Extracts were cleared by centrifugation and diluted with 9 volumes of Low Salt Buffer (Upstate Biotechnology) plus protease inhibitors and the following specific rabbit polyclonal antibodies were added for overnight incubation: anti-FOXM1 (Santa Cruz Biotechnology; K-19, sc-500 X), anti-FOXO1 (anti-FKHR, Santa Cruz Biotechnology; H-128, sc-11350 X), anti-FOXO3A (anti-FKHRL1, Santa Cruz Biotechnology, sc-11351 X), or IgG (2 μg). Protein–DNA complexes were collected with Dynabeads Protein G (Life Technologies) and washed according to the protocol (Upstate Biotechnology). Complexes were dissociated from beads using 1% SDS buffer containing 0.1 mol/L $NaHCO_3$; DNA cross-links were reversed with heat (65°C for 4 hours) and digested with proteinase K for one hour at 37°C. DNA was phenol–chloroform extracted and precipitated with 0.7 volume of 100% isopropanol. Mibefradil-induced enrichment of FOXO1/FOXO3A binding or the loss of FOXM1 binding to specific sites within *BIRC5* promoter was determined on the basis of the absolute quantification in qPCR reaction normalized to the input. Specific primers were designed using Primer3 software (32) and were in proximity to a specific binding site for FOXM1/FOXO binding according to previously published information (Supplementary Table S3; Supplementary Fig. S4E; ref. 33). qPCR was performed using IQ SYBR Green Supermix (Bio-Rad) as follows: one cycle, 3 minutes at 95°C; 40 cycles of 95°C for 15 seconds, 62°C for 30 seconds, and 72°C for 30 seconds.

In vivo human ovarian cancer xenografts

All animal experiments were performed following approval from the Institutional Animal Care and Use Committee at the University of Virginia (Charlottesville, VA). Six to 8-week-old female athymic nude mice (Harlan Laboratories) were injected intraperitoneally with 200 μL PBS containing 10^6 A2780Cis cells stably expressing luciferase following lentiviral transduction, which did not affect cellular response to mibefradil. Tumor-bearing mice were treated in one of 4 arms as follows: (i) 40 mg/kg mibefradil in water via gavage every 6 hours for 5 days (2 cycles); (ii) 25 mg/kg carboplatin in PBS via intraperitoneal injection; (iii) mibefradil and carboplatin as described; or (iv) vehicle control. The dosing schedule was as follows: day 1, inject cells; days 4 to 8 and days 13 to 17, mibefradil, day 9 and 18, carboplatin. The experiment was performed twice with 4 to 5 mice per treatment arm per experiment; the total number of mice analyzed (*n*) is indicated in the figure legends. Mice were observed 2 to 3 times per week by laboratory personnel and monitored for signs of distress (i.e., changes in appearance, respiration, activity, etc.) and weighed; mice showing signs of distress or losing greater than 15% body weight were euthanized and examined for tumor. Tumor burden was assessed in one experiment (n = 4–5 per treatment arm) on days 4, 8, 13, 18, and 24 after tumor cell injection by measuring light emission following intraperitoneal luciferin administration as an indication of luciferase activity using an IVIS imaging system (Molecular Imaging Core, University of Virginia, Charlottesville, VA). Total flux (photons/second) was determined for the entire abdominal cavity per mouse and normalized to the mean total flux of control-treated mice imaged on day 4. Upon experimental termination (day 28), mice were euthanized and tumor burden evaluated upon necropsy by counting the number of tumor nodules and weighing the omentum (primary site of tumor implantation) and any additional tumor nodules. Formalin-fixed, paraffin-embedded tissues were sectioned and H&E stained (University of Virginia Research Histology Core, Charlottesville, VA) to evaluate microscopic tumor burden.

Statistical analysis

All values were expressed as the means of at least three independent experiments ± SEM. Results were compared using one-way ANOVA followed by Tukey multiple comparisons test. $P < 0.05$ indicated statistically significant differences between observed effects. Drug-induced synergy between mibefradil and carboplatin was determined by median dose effect analysis (34) using CompuSyn software (ComboSyn). Combination index (CI) values < 1 denote synergistic interactions. Tumor incidence from the mouse experiments was evaluated using Fisher exact test. All other data from mouse experiments were analyzed using two-way ANOVA followed by Tukey multiple comparisons test.

Results

T-type Ca^{2+} channel expression and sensitivity to inhibition or downregulation in ovarian cancer cells

The contribution of T-type channels to ovarian cancer cell growth was evaluated using a relatively selective antagonist

mibefradil (35) or siRNA knockdown of individual channels. Similar to a previous report (5), qRT-PCR confirmed the expression of the T-type Ca^{2+} channel genes, *CACNA1G* (Cav3.1), *CACNA1H* (Cav3.2), and *CACNA1I* (Cav3.3) in three ovarian cancer cell lines, including A2780, A2780Cis, and IGROV-1, although to different extents (Fig. 1A). Cells were subjected to increasing concentrations of mibefradil for 72 hours, and the viability was determined with the AlamarBlue assay. The results showed that mibefradil decreased cell viability and generated EC_{50} values ranging from 6 to 13 μmol/L (Table 1).

To determine whether mibefradil inhibited proliferation or induced cell death, cells were treated for 24 hours with 10 μmol/L mibefradil and evaluated via trypan blue exclusion. The data showed a 25% to 40% reduction in the total number of cells (Fig. 1B) relative to control mock-treated cells (100%, not shown) for all cell lines. Moreover, the number of viable/live A2780 and A2780Cis cells was 25% of the total, indicating increased cell death. The effects of mibefradil were confirmed using siRNA to individual T-type channels (Supplementary Table S1), where a 35% to 50% decrease in the percentage of live cells was observed in both A2780 and A2780Cis cells (Fig. 1C and Supplementary Fig. S1).

The effects of mibefradil on cell-cycle progression in ovarian cancer cells was examined by treating cells with increasing concentrations of mibefradil for 24 hours. All cell lines showed a dose-dependent decrease in the number of cells in active S-phase (BrdUrd-incorporating) and an increase in the number of cells in G_1 (all cell lines) and/or G_2 (IGROV-1) phases (Fig. 1D). The inhibition of cell-cycle progression after treatment with mibefradil is supported by dose-dependent decreases in the expression of cyclin D1, p27, and Rb as well as decreased Rb phosphorylation, consistent with reduced entry into S-phase (Fig. 1E). These results concur with previously reported induction of G_1 arrest and inhibition of proliferation in A2780 cells treated with T-type channel antagonists (5, 6) or transfected with specific siRNA (5).

Blocking T-type Ca^{2+} channels induced apoptosis in ovarian cancer cells through decreased expression of survivin

In addition to changes in cell-cycle progression, mibefradil treatment promoted a dose-dependent increase in the sub-G_1

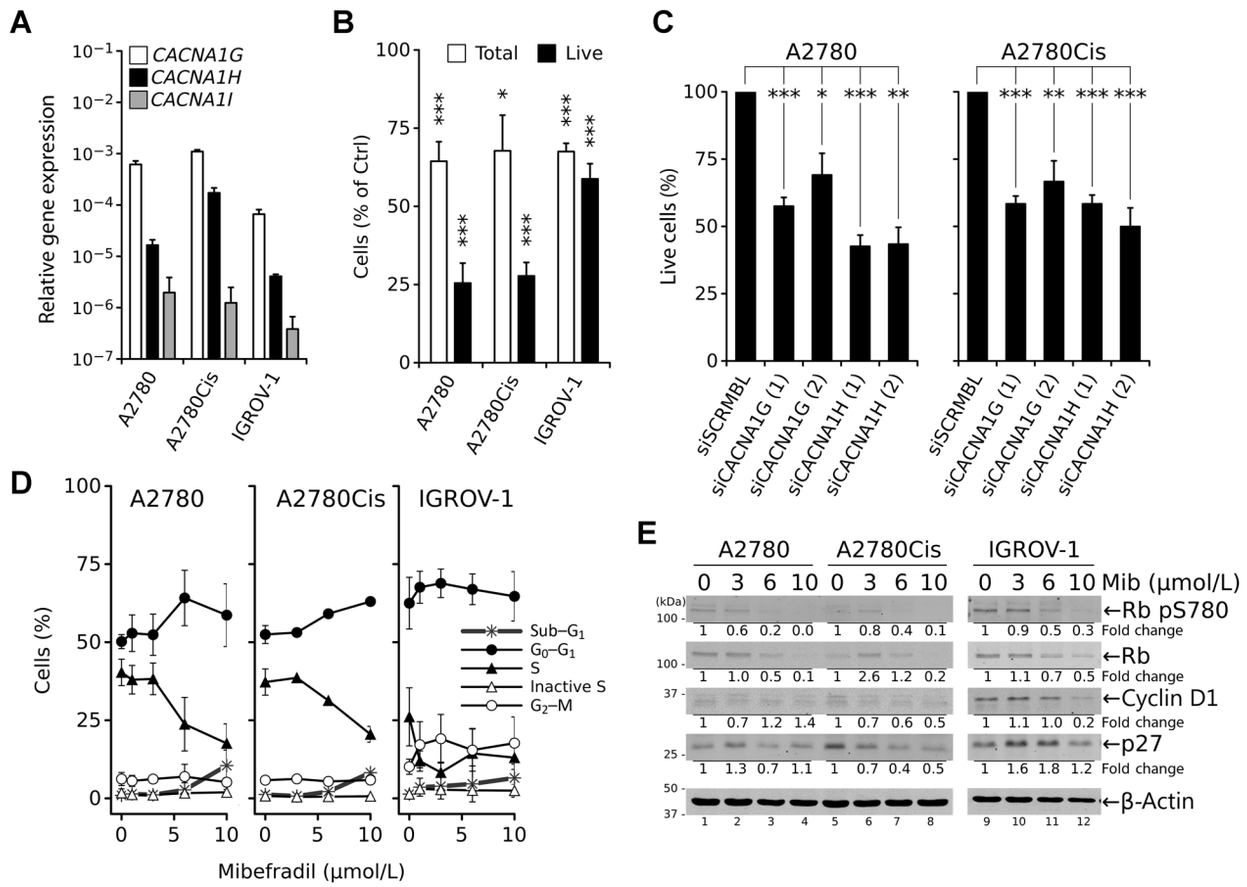

Figure 1.
Ovarian cancer cell lines express T-type Ca^{2+} channels and are sensitive to inhibition. A, expression of mRNA for Cav3.1 (*CACNA1G*), Cav3.2 (*CACNA1H*), and Cav3.3 (*CACNA1I*) in ovarian cancer cell lines normalized to GAPDH expression. B, percentage of total and viable (live, trypan blue–negative) A2780, A2780Cis, and IGROV-1 cells relative to control (100%) after treatment with 10 μmol/L mibefradil for 24 hours. C, percentage of live (trypan blue–negative) A2780 or A2780Cis cells after transfection with siRNA against T-type channel isoforms (two different siRNAs per gene) for 72 hours. D, effects of increasing concentrations of mibefradil on cell cycle in ovarian cancer cells treated for 24 hours. E, Western blot analysis of cell cycle–related proteins in total cell extracts isolated from ovarian cancer cells treated with increasing concentrations of mibefradil (Mib) for 24 hours. All values are the mean ± SEM from ≥ three independent experiments; *, $P < 0.05$; **, $P < 0.01$; ***, $P < 0.001$; NS, $P > 0.05$ relative to untreated or siSCRMBL controls. Ctrl, control.

Table 1. Viability of ovarian cancer cells treated with mibefradil or carboplatin

Cell line	Mibefradil $EC_{50} \pm$ SEM (μmol/L)	Carboplatin $EC_{50} \pm$ SEM (μg/mL)
A2780	6.6 ± 0.7	5.9 ± 0.83
A2780Cis	7.7 ± 0.8	19 ± 2.3
IGROV-1	9.6 ± 0.8	14 ± 2.1
SKOV3.ip1	13 ± 2.2	18 ± 3.3

NOTE: Cells were treated with mibefradil continuously for 72 hours, and the viability was determined by alamarBlue assay as described (see Material and Methods). Values represent the average of ≥ three independent experiments ± SEM. EC_{50}, drug concentration that decreased viability by 50%.

population (Figs. 1D and 2A). Treatment with 10 μmol/L mibefradil for 24 hours also increased cleaved PARP, caspase-9, and caspase-7 (Fig. 2B), well-established markers of apoptosis, and reduced expression of survivin, an antiapoptotic factor. Indeed, survivin protein (Fig. 2B) and mRNA (*BIRC5*; Fig. 2C) levels decreased 20% to 60% and 30% to 50%, respectively, following 24 hours of treatment with 10 μmol/L mibefradil relative to untreated cells. Furthermore, reduced *CACNA1G* or *CACNA1H* expression following transfection with two different siRNA oligomers directed against each gene diminished survivin (Supplementary Fig. S2) and *BIRC5* expression (Fig. 2D) approximately 30% to 50% relative to control cells (siSCRMBL).

Inhibition of T-type Ca^{2+} channels targeted the PI3K/AKT pathway and forkhead box transcription factors

One mechanism that regulates survivin gene expression depends on forkhead box transcription factors: FOXM1 acting as an activator (36) and FOXO proteins (FOXO3A and/or FOXO1) acting as repressors (33). FOXO proteins, in turn, are regulated by PI3K/AKT pathway (37). To determine whether T-type Ca^{2+} channels regulated survivin gene expression through this pathway, ovarian cancer cells were treated with increasing concentrations of mibefradil and examined for AKT phosphorylation and changes in expression of FOXM1 and FOXO proteins. As demonstrated in Fig. 3A, mibefradil modestly reduced basal AKT phosphorylation and FOXM1 protein expression in A2780Cis and IGROV-1 cells in a concentration-dependent manner. The mibefradil-dependent reduction of FOXM1 expression in IGROV-1 cells was more obvious in the nuclear fraction (Fig. 3C). Mibefradil also increased basal levels and nuclear retention of FOXO1 protein in IGROV-1 cells (Fig. 3A and C) and FOXO3A protein in A2780Cis cells (not shown). Mibefradil had a more pronounced effect on stimulated expression. Stimulation of serum-starved A2780Cis and IGROV-1 cells with insulin (10 μg/mL) for increasing periods of time produced maximal phosphorylation of AKT in both cell lines within 15 minutes, which was maintained for 8 hours (Fig. 3B). Pretreatment with mibefradil (10 μmol/L for 60 minutes) delayed peak AKT phosphorylation to 1 hour and decreased the time during which it was

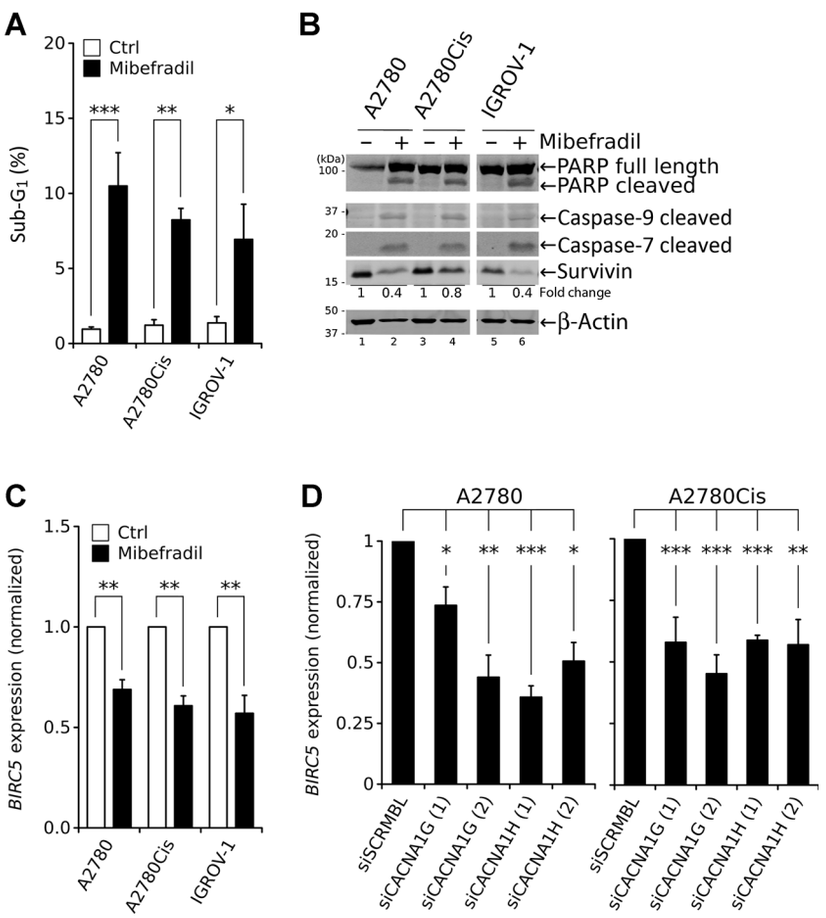

Figure 2.
Inhibition of T-type Ca^{2+} channels induces apoptosis and lowers survivin expression in ovarian cancer cells. A, sub-G_1 population in cells treated with 10 μmol/L mibefradil for 24 hours was determined by flow cytometry. B, Western blot analysis of markers of apoptotic cell death in total cell extracts from ovarian cancer cells treated with 10 μmol/L mibefradil for 24 hours. C, expression of *BIRC5* mRNA determined by quantitative RT-PCR in ovarian cancer cells treated with mibefradil for 24 hours at 6 μmol/L (A2780) or 10 μmol/L (A2780Cis and IGROV-1). D, expression of *BIRC5* mRNA determined by quantitative RT-PCR in A2780 and A2780Cis cells 72 hours after transfection with siRNA against T-type channels isoforms. All values are the mean ± SEM from ≥ two independent experiments; *, $P < 0.05$; **, $P < 0.01$; ***, $P < 0.001$. Ctrl, control.

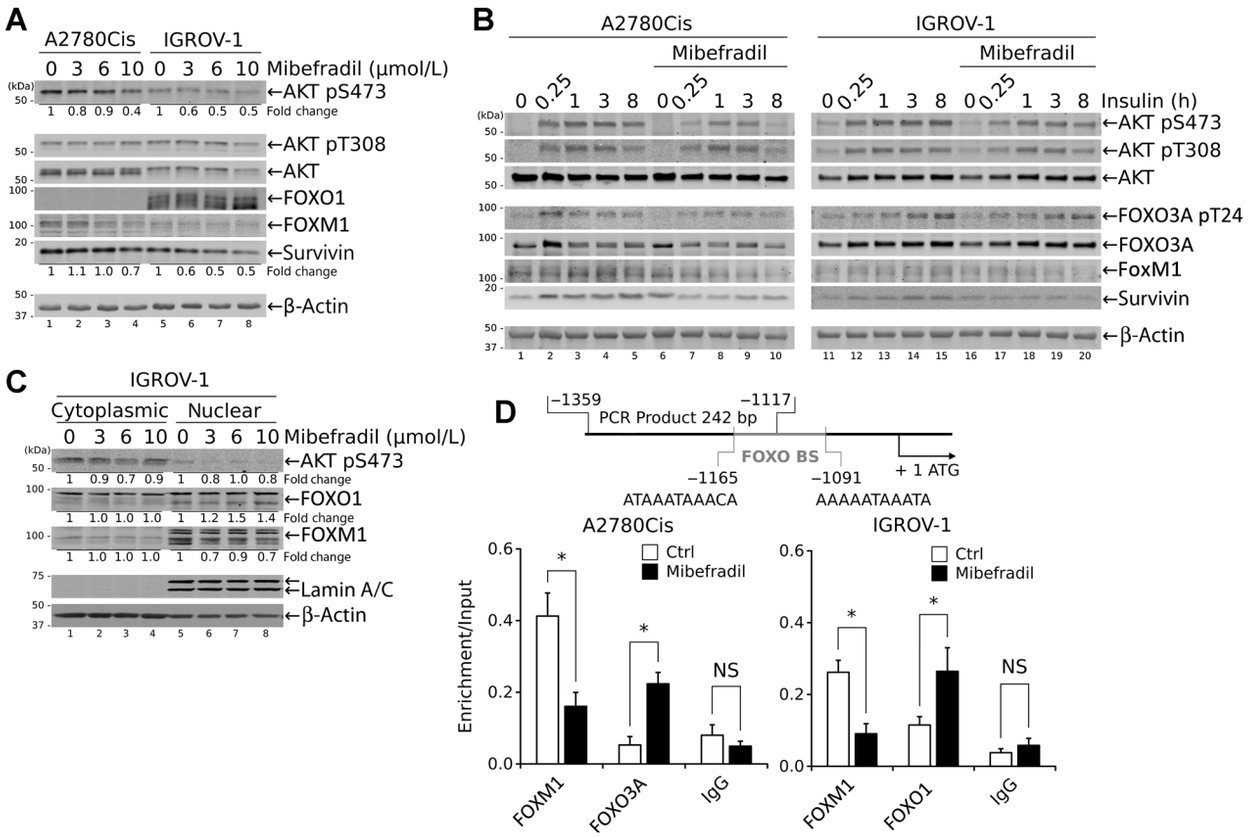

Figure 3.

Treatment with mibefradil reduces survivin expression in ovarian cancer cells through disruption of PI3K/AKT and forkhead box protein activities and subcellular localization. A, A2780Cis and IGROV-1 cells were treated with the indicated concentrations of mibefradil for 24 hours prior to blotting for AKT phosphorylation and FOXO1 and FOXM1 protein expression. B, cells were treated with 10 μmol/L mibefradil for 1 hour followed by stimulation with 10 μg/mL insulin for up to 8 hours. C, subcellular localization of FOXO1 and FOXM1 was determined by blotting cytoplasmic or nuclear extracts of IGROV-1 cells treated with increasing concentrations of mibefradil for 24 hours. D, A2780Cis cells or IGROV-1 cells were treated with mibefradil (10 μmol/L) or DMSO for 24 hours, cross-linked, and subjected to ChIP using antibodies specific for the indicated proteins; rabbit IgG served as a negative control. Enrichment in the binding of specific proteins was determined based on the amplification of immunoprecipitated DNA by qPCR of the *BIRC5* promoter using specific primers spanning the FOXO binding sites (FOXO BS; schematic on top). The data were normalized to the corresponding input DNA as described (see Materials and Methods) and are presented as the mean from two independent experiments ± SEM; *, $P < 0.05$. Ctrl, control.

maintained (Fig. 3B). Mibefradil treatment inhibited insulin-stimulated AKT activity as evidenced by reduced phosphorylation of GSK-3β and PRAS40 (Supplementary Fig. S3A), direct substrates of AKT. Similarly, FOXO3A phosphorylation (A2780Cis), FOXM1, and survivin expression were reduced with mibefradil pretreatment of insulin-stimulated cells (Fig. 3B). Conversely, treatment with the serine/threonine phosphatase inhibitor calyculin A prevented the loss of AKT phosphorylation and preserved FOXM1 and survivin expression following mibefradil treatment (Supplementary Fig. S3B). Together, the data demonstrate that mibefradil suppresses activation of the PI3K/AKT pathway, resulting in increased protein expression and nuclear retention of FOXO1 and/or FOXO3A and decreased FOXM1 protein expression, all of which have been implicated in the transcriptional suppression of *BIRC5* expression.

Mibefradil inhibits *BIRC5* transcription by regulating promoter occupancy

FOXO proteins regulate *BIRC5* expression through direct binding to the promoter (Fig. 3D; refs. 36, 38). Suppression of *BIRC5* expression is associated with the loss of FOXM1, a transcriptional activator and recruitment of transcriptional repressors, including FOXO1 and FOXO3A (38), which in turn bind histone deacetylases (HDAC) to facilitate chromatin remodeling (reviewed in ref. 20). To investigate whether inhibition of *BIRC5* expression occurs at the level of chromatin, we analyzed the binding of transcriptional regulators to the *BIRC5* promoter using ChIP and specific antibodies for FOXM1, FOXO3A, or FOXO1. Treatment of A2780Cis cells or IGROV-1 cells with mibefradil (10 μmol/L) resulted in a significant decrease in FOXM1 binding to the *BIRC5* promoter as compared with DMSO-treated control (Fig. 3D). At the same time, mibefradil treatment increased specific binding of the transcriptional repressors FOXO3A (A2780Cis) or FOXO1 (IGROV-1) to the *BIRC5* promoter (Fig. 3D). These data, together with the previous observations that mibefradil treatment decreased survivin mRNA (Fig. 2C and D) and protein expression (Fig. 2B and Fig. 3A), support the notion that T-type Ca^{2+} channels regulate survivin gene expression by controlling AKT activity and the binding of FOXM1/FOXO proteins within the *BIRC5* promoter.

Mibefradil synergized with carboplatin to inhibit ovarian cancer cell growth *in vitro*

The drug-induced decrease in expression of the antiapoptotic protein, survivin, as well as the suppression of AKT/FOXM1 and the activation of FOXO signaling pathways are valid circuitry for anticancer drug intervention (39). For women with advanced stage ovarian cancer, platinum resistance is one of the major obstacles impairing successful treatment. Therefore, we investigated the ability of mibefradil to act as a sensitizing agent to carboplatin using selected ovarian cancer cells *in vitro*. Cells were treated with increasing concentrations of mibefradil (0–10 μmol/L) for 24 hours, followed by incubation for another 24 hours in fresh media or media with the indicated concentrations of carboplatin (Fig. 4A). With the exception of SKOV3.ip1, mibefradil alone inhibited growth of all cell lines to varying degrees (Fig. 4A). Pretreatment of ovarian cancer cells with mibefradil increased the response to sublethal concentrations of carboplatin (Table 1) in a dose-dependent manner in all cell lines with the exception of SKOV3.ip1 (Fig. 4A). The growth of A2780Cis cells was inhibited approximately 20% following treatment with either 3 μmol/L of mibefradil or 1 to 3 μg/mL of carboplatin (EC_{50} = 19 ± 2.3 μg/mL, Table 1) alone; sequential treatment of mibefradil (3 μmol/L) followed by carboplatin (1 or 3 μg/mL) resulted in 50% growth inhibition (Fig. 4A). Similarly IGROV-1 or OVCAR-3 cells treated with mibefradil (3 μmol/L) or carboplatin (1 or 3 μg/mL) showed marginal growth inhibition (~10%), while the combination resulted in greater than 50% growth inhibition (Fig. 4A). However, A2780 cells were sensitive to carboplatin (50% decrease with 1 μg/mL), which was modestly affected by pretreatment with mibefradil, and ES2 cells showed a dose-dependent decrease in growth with mibefradil alone that was marginally affected by the addition of carboplatin (Fig. 4A). To determine whether the growth-inhibitory effects

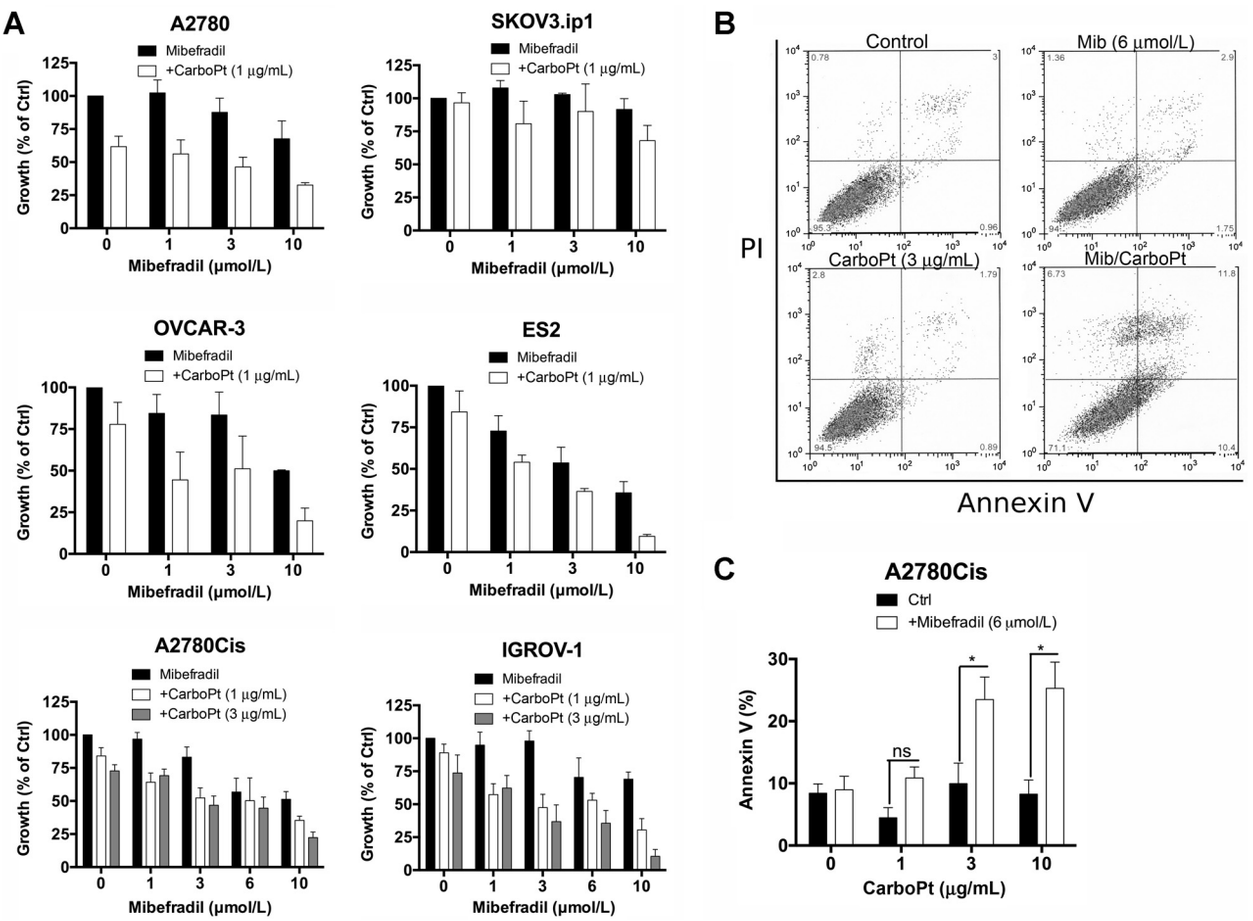

Figure 4.
T-type Ca^{2+} channel inhibitor mibefradil (Mib) sensitizes ovarian cancer cells to carboplatin (CarboPt). A, A2780, SKOV3.ip1, OVCAR3, ES2, A2780Cis, or IGROV-1 cells were treated with the indicated concentrations of mibefradil for 24 hours, followed by 24 hours of treatment with the indicated concentrations of carboplatin, and the growth was determined by CyQUANT assay (for A2780, SKOV3.ip1, OVCAR-3, and ES2 cells) and SRB assay (for A2780Cis and IGROV-1). Graphs represent data from ≥ two independent experiments ± SEM. B, representative histograms of A2780Cis cells treated for 24 hours with mibefradil (Mib; 6 μmol/L), carboplatin (CarboPt; 3 μg/mL), or the combination of both and stained for Annexin V and PI. C, quantification of apoptosis induction in A2780Cis cells by the combined treatment of mibefradil (6 μmol/L) and carboplatin (1, 3, or 10 μg/mL), as measured by Annexin V-FITC/PI staining. The percentage of apoptotic cells includes a sum of the early apoptosis (bottom right quadrant) and late apoptotic cells (top right quadrant). Graph represents data from > three independent experiments ± SEM; *, $P < 0.05$; ns, not significant. Ctrl, control.

were synergistic or additive, the Chou–Talalay method was used to obtain CIs (Supplementary Table S4); values lower than one indicate drug synergy, whereas those close to one indicate additive effects (34). The analysis indicated drug synergy for A2780Cis, IGROV-1, and OVCAR-3 cells, while the effects of mibefradil and carboplatin were additive in SKOV-3.ip1, A2780, and ES2 cells (Supplementary Table S4). The synergistic growth inhibition induced by mibefradil and carboplatin was likely due to an increase in apoptosis. A2780Cis cells, treated with mibefradil and carboplatin for 24 hours, induced a significantly high level of apoptosis (~25%) compared with the control, as measured by Annexin V-FITC/7-AAD staining (Fig. 4B and C) and PARP cleavage (Supplementary Fig. S4A and S4C); neither mibefradil (6 μmol/L) nor carboplatin (0.1–30 μg/mL) alone stimulated apoptosis above control (Fig. 4B and C; Supplementary Fig. S4A and S4C). Mibefradil treatment or reduced expression of *CACNA1G* or *CACNA1H*, but not carboplatin, decreased survivin expression, and no further decrease was observed when combined; however, the combination increased γH2AX (Supplementary Fig. S4), indicating an increase in DNA double-strand breaks that was not observed with mibefradil or carboplatin alone.

Mibefradil improved the response of peritoneal ovarian cancer growth to carboplatin in a mouse model

Intraperitoneal injection of human ovarian cancer cells into nude mice mimics many aspects of stage III ovarian cancer, including extensive peritoneal dissemination and the development of ascites. This model was employed to evaluate whether mibefradil sensitizes ovarian cancer cells to carboplatin *in vivo*. Following intraperitoneal injection of comparatively platinum-resistant, luciferase-expressing A2780Cis cells, mice were divided into 4 treatment arms: mibefradil alone, carboplatin alone, mibefradil followed by carboplatin, or vehicle control. Three days after tumor initiation, mice received daily injections of mibefradil or vehicle for 5 days followed by a single dose of carboplatin or vehicle; this schedule was repeated 3 days after the carboplatin dosing (see Materials and Methods; Fig. 5A). Bioluminescent imaging was performed prior to treatment on the indicated days (Fig. 5A and B) and revealed an increase in tumor growth over time for all groups (Fig. 5B). However, mice that received the combination treatment showed a significant reduction in light emission compared with control or either single-treatment arm (Fig. 5B). Upon necropsy, visible tumor nodules were observed throughout the peritoneal cavity and most prominently on the

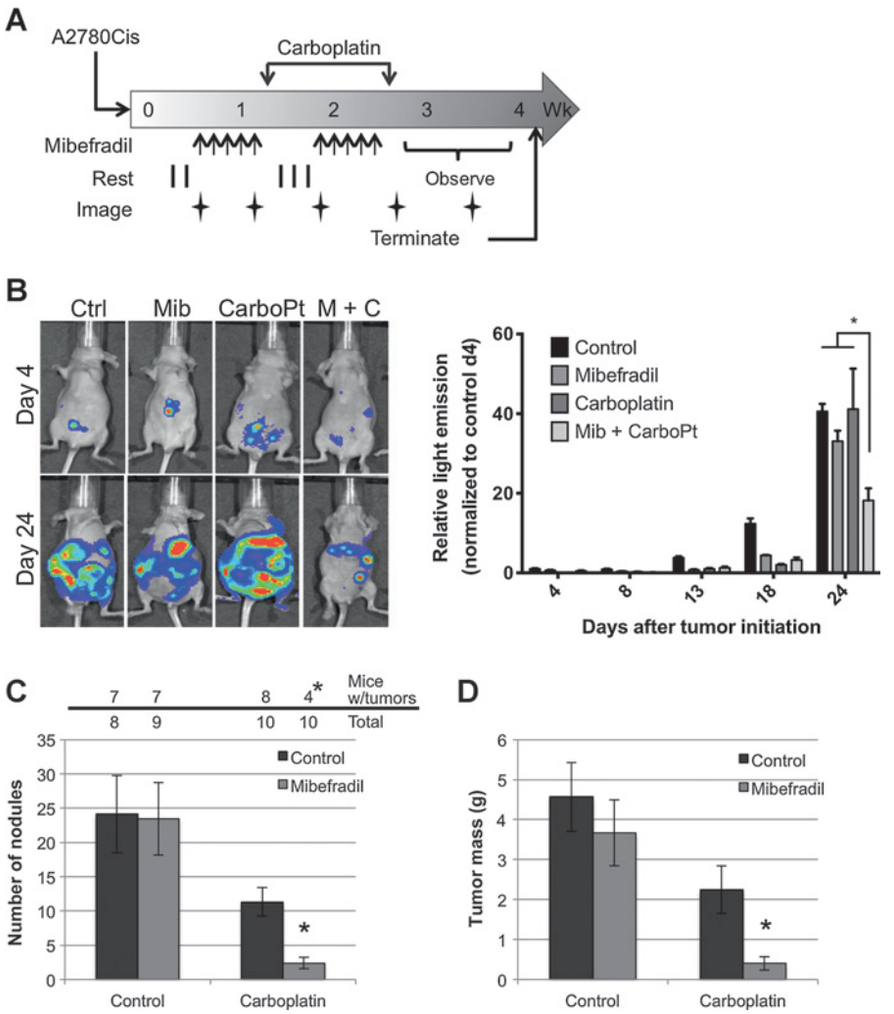

Figure 5.
Mibefradil sensitizes human ovarian cancer cells to carboplatin (carboPt) in a mouse model of peritoneal metastasis. A, schematic representation of treatment protocol. Mice were injected with 10^6 A2780Cis cells (day 0), treated daily with mibefradil days 4–8 and 13–17 (arrows), and twice with carboplatin one day following the last dose of mibefradil (days 9 and 18). Whole-body images of light emission were obtained on days 4, 8, 13, 18, and 24. Imaging was performed prior to administration of treatment. B, left panel depicts representative luminescent images from individual mice in each of the 4 treatment groups taken on days 4 and 24. Total light emission was obtained from each of 4 mice per treatment arm on the indicated days after tumor initiation; values were normalized to images of control (Ctrl)-treated mice taken on day 4 (right). Data, mean ± SEM; *, $P < 0.05$ determined by two-way ANOVA, followed by Tukey multiple comparisons test. C, tumor incidence (top). The number of mice with visible tumor nodules at necropsy and the total number of mice per treatment arm are indicated. *, $P < 0.05$ determined with Fisher exact test. Bottom, tumor nodules. The number of macroscopic tumor nodules was counted from each mouse upon necropsy. Data, mean nodule count ± SEM; *, $P < 0.05$, determined by two-way ANOVA, followed by Tukey multiple comparisons test. D, tumor weight. The omentum, mesentary, and any visible tumor nodules were removed from each mouse and weighed. Data, mean tumor weight ± SEM; *, $P < 0.05$, determined by two-way ANOVA followed by Tukey multiple comparisons test. Mib, mibefradil; CarboPt, carboplatin; M + C, mibefradil + carboplatin.

omentum and mesenteric fat in greater than 75% of the mice in the control or single-treatment arms compared with only 40% of the mice treated with both mibefradil and carboplatin (Fig. 5C). Mice receiving mibefradil plus carboplatin had an average of 3 visible tumor nodules within the peritoneum compared with 24 for control or mibefradil alone and 11 for carboplatin alone (Fig. 5C). Although the number of tumor nodules in the carboplatin-treated mice was lower than control, the difference was not statistically significant. As an additional measure of tumor burden, the omentum, mesentery, and visible tumor nodules were dissected from surrounding tissue and weighed. The tumor weight in mice receiving the dual treatment was 0.41 ± 0.17 g, which was significantly lower than control (4.56 ± 0.86) or either single treatment (mibefradil, 3.67 ± 0.82 and carboplatin, 2.25 ± 0.59; Fig. 5D). Again, the difference between carboplatin treatment alone and control was not significant. Together, these observations demonstrate that mibefradil enhanced the response of relatively resistant cells to carboplatin *in vivo*, thus supporting the sensitization data observed *in vitro* and indicating that combination therapy might be effective in treating women with ovarian cancer.

Discussion

The lack of effective therapeutics for the treatment of ovarian cancer has hampered the ability to improve prognosis for women diagnosed with this disease. Cytotoxic platinum-based agents, such as cisplatin and carboplatin, are an important part of first-line therapy in patients suffering from epithelial ovarian cancer. Unfortunately, the anticancer activity of platinum agents is impaired by tumor chemoresistance, either intrinsic or acquired. In effect, over 90% of patients with advanced recurrent ovarian cancer will die because of chemotherapeutic resistance. In this study, we found that blocking T-type Ca^{2+} channels with a chemical antagonist or decreasing expression with siRNA reduced proliferation, induced proapoptotic responses, and sensitized ovarian cancer cells to carboplatin *in vitro*. Most importantly, the T-type channel antagonist mibefradil enhanced antitumor activity of carboplatin *in vivo*.

Blocking T-type channels in ovarian cancer cells produced (i) a cytostatic, antiproliferative effect blocking cell growth in the G_1 and/or G_2 phases of the cell cycle and (ii) a cytotoxic, lethal effect associated with features of apoptosis (increase in sub-G_1 population and cleavage of PARP, caspase-9, and caspase-7). These effects were independent of histopathologic subtype (40) or p53 status (40–42) of the cells. Growth inhibition and G_1 arrest, following treatment with an antagonist or transfection with siRNA targeting T-type channels, have been reported (5), and the induction of apoptosis has been shown in ovarian cancer cells treated with KYS05090, a structurally dissimilar T-type channel antagonist (6). However, the detailed mechanism for the induction of those effects has not been elucidated. The data presented here demonstrate that blocking T-type channels induces caspase-dependent apoptosis (Fig. 2B) associated with decreased survivin mRNA and protein expression (Fig. 2B and C).

Survivin is thought to be one of the most important antiapoptotic factors in cancer cells. It is often overexpressed in ovarian cancers [in more than 70% of cases (15)] and correlates with poor prognostic parameters, such as high grade, histopathologic type, p53 mutation, increased proliferation, and chemoresistance (13, 15, 16, 18). Kaplan–Meier survival analysis demonstrated that the patients with tumors overexpressing survivin have a short overall survival (16). As a result, inhibitors of survivin expression have been developed and tested in clinical trials, although with limited success (43–46).

Survivin is a direct downstream target of the PI3K/AKT pathway through FOXO transcription factors. Activation of the PI3K/AKT pathway results the in inactivation of FOXO-containing transcription repressor complexes and increased expression of survivin (33, 47). Indeed, mibefradil treatment decreased AKT phosphorylation and increased FOXO protein levels in ovarian cancer cells (Fig. 3). Furthermore, blocking T-type Ca^{2+} channels decreased FOXM1 expression. FOXM1 is often overexpressed in ovarian tumors (48), and its transcriptional levels increase with tumor grade, suggesting a role in the progression of ovarian cancer (49). Although blocking T-type Ca^{2+} channels inhibits PI3K/AKT signaling to FOXO and reduces survivin expression, the direct molecular connection between T-type channels and PI3K/AKT/FOXO pathway is still unknown and likely involves Ca^{2+}-dependent pathways.

The inhibition of survivin expression enhances the ability of platinum agents to induce apoptosis and increase DNA double-strand breaks in ovarian cancer and non–small cell lung cancer cells (43, 50). The ability of mibefradil to decrease survivin expression is consistent with the notion that it primes cells for apoptosis induced by chemotherapeutic agents, such as carboplatin. Indeed, treatment of ovarian cancer cells with both carboplatin and mibefradil increased cytotoxicity and drug synergy (Fig. 4; Supplementary Table S4). Interestingly, mibefradil and carboplatin synergistically inhibited the growth of platinum-resistant A2780Cis and IGROV-1 cells, while the inhibition of platinum-sensitive A2780 cells was mildly synergistic (Fig. 4), perhaps because each agent alone is capable of inhibiting growth at low drug concentrations. Although the combination had no additional effect on survivin expression, the treatment with mibefradil and carboplatin increased DNA double-strand breaks (Supplementary Fig. S4C). Importantly, adding mibefradil pretreatment to carboplatin-based therapy *in vivo* resulted in a significant reduction in xenograft tumor burden in mice harboring platinum-resistant tumors (Fig. 5). This has important implications for the treatment of ovarian cancer patients who frequently succumb to platinum-resistant disease. Thus, the data presented here support the use of T-type Ca^{2+} channel blockers, either alone or together with platinum agents in the treatment of ovarian cancer patients.

Disclosure of Potential Conflicts of Interest

L.S. Gray is a consultant for, has ownership interest (including patents) in, and is a consultant/advisory board member for Cavion. J. Dziegielewski reports receiving a commercial research grant from and is a consultant for Cavion. No potential conflicts of interest were disclosed by the other authors..

Authors' Contributions

Conception and design: B. Dziegielewska, L.S. Gray, J. Dziegielewski, J.K. Slack-Davis

Development of methodology: B. Dziegielewska, E.V. Casarez, J. Dziegielewski, J.K. Slack-Davis

Acquisition of data (provided animals, acquired and managed patients, provided facilities, etc.): E.V. Casarez, W.Z. Yang, J. Dziegielewski, J.K. Slack-Davis

Analysis and interpretation of data (e.g., statistical analysis, biostatistics, computational analysis): B. Dziegielewska, E.V. Casarez, W.Z. Yang, J. Dziegielewski, J.K. Slack-Davis

Writing, review, and/or revision of the manuscript: B. Dziegielewska, W.Z. Yang, J. Dziegielewski, J.K. Slack-Davis

Administrative, technical, or material support (i.e., reporting or organizing data, constructing databases): E.V. Casarez, J.K. Slack-Davis
Study supervision: J.K. Slack-Davis

Grant Support

This study was supported in part by the University of Virginia Women's Oncology Research Fund, Commonwealth Foundation for Cancer Research, NCI grant R01 CA142783 (to J.K. Slack-Davis and E.V. Casarez), George Amorino Pilot Grant from the UVA Department of Radiation Oncology (to B. Dziegielewska), and Cavion LLC research grant (to J. Dziegielewski). This work used IVIS bioluminescence scanner in the Molecular Imaging Core, which was purchased with support from NIH grant 1S10RR025694-01, and resources from the Flow Cytometry Core Facility and Research Histology Core. All cores are supported by the University of Virginia School of Medicine and the Cancer Center.

The costs of publication of this article were defrayed in part by the payment of page charges. This article must therefore be hereby marked *advertisement* in accordance with 18 U.S.C. Section 1734 solely to indicate this fact.

Received June 2, 2015; revised December 22, 2015; accepted December 23, 2015; published OnlineFirst February 1, 2016.

References

1. Siegel RL, Miller KD, Jemal A. Cancer statistics, 2015. CA Cancer J Clin 2015;65:5–29.
2. Clapham DE. Calcium signaling. Cell 2007;131:1047–58.
3. Monteith GR, Davis FM, Roberts-Thomson SJ. Calcium channels and pumps in cancer: changes and consequences. J Biol Chem 2012;287:31666–73.
4. Perez-Reyes E. Molecular physiology of low-voltage-activated t-type calcium channels. Physiol Rev 2003;83:117–61.
5. Li W, Zhang S-L, Wang N, Zhang B-B, Li M. Blockade of T-type Ca(2+) channels inhibits human ovarian cancer cell proliferation. Cancer Invest 2011;29:339–46.
6. Jang SJ, Choi HW, Choi DL, Cho S, Rim H-K, Choi H-E, et al. *In vitro* cytotoxicity on human ovarian cancer cells by T-type calcium channel blockers. Bioorg Med Chem Lett 2013;23:6656–62.
7. Valerie NCK, Dziegielewska B, Hosing AS, Augustin E, Gray LS, Brautigan DL, et al. Inhibition of T-type calcium channels disrupts Akt signaling and promotes apoptosis in glioblastoma cells. Biochem Pharmacol 2013;85:888–97.
8. Dziegielewska B, Brautigan DL, Larner JM, Dziegielewski J. T-type Ca2+ channel inhibition induces p53 dependent cell growth arrest and apoptosis through activation of p38-MAPK in colon cancer cells. Mol Cancer Res 2014;12:348–58.
9. Altieri DC. Survivin, versatile modulation of cell division and apoptosis in cancer. Oncogene 2003;22:8581–9.
10. Altieri DC. Survivin - The inconvenient IAP. Semin Cell Dev Biol 2015;39:91–6.
11. Wang Q, Chen Z, Diao X, Huang S. Induction of autophagy-dependent apoptosis by the survivin suppressant YM155 in prostate cancer cells. Cancer Lett 2011;302:29–36.
12. Capalbo G, Dittmann K, Weiss C, Reichert S, Hausmann E, Rödel C, et al. Radiation-induced survivin nuclear accumulation is linked to DNA damage repair. Int J Radiat Oncol Biol Phys 2010;77:226–34.
13. Aune G, Stunes AK, Tingulstad S, Salvesen O, Syversen U, Torp SH. The proliferation markers Ki-67/MIB-1, phosphohistone H3, and survivin may contribute in the identification of aggressive ovarian carcinomas. Int J Clin Exp Pathol 2011;4:444–53.
14. Chen L, Liang L, Yan X, Liu N, Gong L, Pan S, et al. Survivin status affects prognosis and chemosensitivity in epithelial ovarian cancer. Int J Gynecol Cancer 2013;23:256–63.
15. Cohen C, Lohmann CM, Cotsonis G, Lawson D, Santoianni R. Survivin expression in ovarian carcinoma: correlation with apoptotic markers and prognosis. Mod Pathol 2003;16:574–83.
16. Sui L, Dong Y, Ohno M, Watanabe Y, Sugimoto K, Tokuda M. Survivin expression and its correlation with cell proliferation and prognosis in epithelial ovarian tumors. Int J Oncol 2002;21:315–20.
17. Zaffaroni N, Pennati M, Colella G, Perego P, Supino R, Gatti L, et al. Expression of the anti-apoptotic gene survivin correlates with taxol resistance in human ovarian cancer. Cell Mol Life Sci 2002;59:1406–12.
18. Rödel F, Sprenger T, Kaina B, Liersch T, Rödel C, Fulda S, et al. Survivin as a prognostic/predictive marker and molecular target in cancer therapy. Curr Med Chem 2012;19:3679–88.
19. Altieri DC. Targeting survivin in cancer. Cancer Lett 2013;332:225–8.
20. Boidot R, Végran F, Lizard-Nacol S. Transcriptional regulation of the survivin gene. Mol Biol Rep 2014;41:233–40.
21. Nogueira-Ferreira R, Vitorino R, Ferreira-Pinto MJ, Ferreira R, Henriques-Coelho T. Exploring the role of post-translational modifications on protein-protein interactions with survivin. Arch Biochem Biophys 2013;538:64–70.
22. Stauber RH, Mann W, Knauer SK. Nuclear and cytoplasmic survivin: molecular mechanism, prognostic, and therapeutic potential. Cancer Res 2007;67:5999–6002.
23. Ning Y, Li Q, Xiang H, Liu F, Cao J. Apoptosis induced by 7-difluoromethoxyl-5,4′-di-n-octyl genistein via the inactivation of FoxM1 in ovarian cancer cells. Oncol Rep 2012;27:1857–64.
24. Jiang L, Cao X-C, Cao J-G, Liu F, Quan M-F, Sheng X-F, et al. Casticin induces ovarian cancer cell apoptosis by repressing FoxM1 through the activation of FOXO3a. Oncol Lett 2013;5:1605–10.
25. Obexer P, Hagenbuchner J, Unterkircher T, Sachsenmaier N, Seifarth C, Böck G, et al. Repression of BIRC5/survivin by FOXO3/FKHRL1 sensitizes human neuroblastoma cells to DNA damage-induced apoptosis. Mol Biol Cell 2009;20:2041–8.
26. Chakrabarty A, Bhola NE, Sutton C, Ghosh R, Kuba MG, Dave B, et al. Trastuzumab-resistant cells rely on a HER2-PI3K-FoxO-survivin axis and are sensitive to PI3K inhibitors. Cancer Res 2013;73:1190–200.
27. Yang X, Zheng F, Xing H, Gao Q, Wei W, Lu Y, et al. Resistance to chemotherapy-induced apoptosis via decreased caspase-3 activity and overexpression of antiapoptotic proteins in ovarian cancer. J Cancer Res Clin Oncol 2004;130:423–8.
28. Church DN, Talbot DC. Survivin in solid tumors: rationale for development of inhibitors. Curr Oncol Rep 2012;14:120–8.
29. Mariot P, Vanoverberghe K, Lalevee N, Rossier MF, Prevarskaya N. Overexpression of an alpha 1H (Cav3.2) T-type calcium channel during neuroendocrine differentiation of human prostate cancer cells. J Biol Chem 2002;277:10824–33.
30. Bustin SA, Benes V, Garson JA, Hellemans J, Huggett J, Kubista M, et al. The MIQE guidelines: minimum information for publication of quantitative real-time PCR experiments. Clin Chem 2009;55:611–22.
31. Zhu N, Gu L, Findley HW, Chen C, Dong J-T, Yang L, et al. KLF5 Interacts with p53 in regulating survivin expression in acute lymphoblastic leukemia. J Biol Chem 2006;281:14711–8.
32. Untergasser A, Cutcutache I, Koressaar T, Ye J, Faircloth BC, Remm M, et al. Primer3–new capabilities and interfaces. Nucleic Acids Res 2012;40:e115.
33. Guha M, Plescia J, Leav I, Li J, Languino LR, Altieri DC. Endogenous tumor suppression mediated by PTEN involves survivin gene silencing. Cancer Res 2009;69:4954–8.
34. Chou TC, Talalay P. Quantitative analysis of dose-effect relationships: the combined effects of multiple drugs or enzyme inhibitors. Adv Enzyme Regul 1984;22:27–55.
35. Mishra SK, Hermsmeyer K. Selective inhibition of T-type Ca2+ channels by Ro 40-5967. Circ Res 1994;75:144–8.
36. Wang I-C, Chen Y-J, Hughes D, Petrovic V, Major ML, Park HJ, et al. Forkhead box M1 regulates the transcriptional network of genes essential for mitotic progression and genes encoding the SCF (Skp2-Cks1) ubiquitin ligase. Mol Cell Biol 2005;25:10875–94.
37. Brunet A, Bonni A, Zigmond MJ, Lin MZ, Juo P, Hu LS, et al. Akt promotes cell survival by phosphorylating and inhibiting a Forkhead transcription factor. Cell 1999;96:857–68.
38. Guha M, Altieri DC. Survivin as a global target of intrinsic tumor suppression networks. Cell Cycle 2009;8:2708–10.
39. Zhou J, Wang Y, Wang Y, Yin X, He Y, Chen L, et al. FOXM1 modulates cisplatin sensitivity by regulating EXO1 in ovarian cancer. PLoS ONE 2014;9:e96989.

40. Domcke S, Sinha R, Levine DA, Sander C, Schultz N. Evaluating cell lines as tumour models by comparison of genomic profiles. Nat Commun 2013;4:2126.
41. Muscolini M, Montagni E, Caristi S, Nomura T, Kamada R, Di Agostino S, et al. Characterization of a new cancer-associated mutant of p53 with a missense mutation (K351N) in the tetramerization domain. Cell Cycle 2009;8:3396–405.
42. Yaginuma Y, Westphal H. Abnormal structure and expression of the p53 gene in human ovarian carcinoma cell lines. Cancer Res 1992; 52:4196–9.
43. Mir R, Stanzani E, Martinez-Soler F, Villanueva A, Vidal A, Condom E, et al. YM155 sensitizes ovarian cancer cells to cisplatin inducing apoptosis and tumor regression. Gynecol Oncol 2014;132:211–20.
44. Lewis KD, Samlowski W, Ward J, Catlett J, Cranmer L, Kirkwood J, et al. A multi-center phase II evaluation of the small molecule survivin suppressor YM155 in patients with unresectable stage III or IV melanoma. Invest New Drugs 2011;29:161–6.
45. Kelly RJ, Thomas A, Rajan A, Chun G, Lopez-Chavez A, Szabo E, et al. A phase I/II study of sepantronium bromide (YM155, survivin suppressor) with paclitaxel and carboplatin in patients with advanced non-small-cell lung cancer. Ann Oncol 2013;24:2601–6.
46. Wiechno P, Somer BG, Mellado B, Chøosta PL, Cervera Grau JM, Castellano D, et al. A randomised phase 2 study combining LY2181308 sodium (survivin antisense oligonucleotide) with first-line docetaxel/prednisone in patients with castration-resistant prostate cancer. Eur Urol 2014;65:516–20.
47. Dansen TB, Burgering BMT. Unravelling the tumor-suppressive functions of FOXO proteins. Trends Cell Biol 2008;18:421–9.
48. Cancer Genome Atlas Research Network. Integrated genomic analyses of ovarian carcinoma. Nature 2011;474:609–15.
49. Llauradó M, Majem B, Castellví J, Cabrera S, Gil-Moreno A, Reventós J, et al. Analysis of gene expression regulated by the ETV5 transcription factor in OV90 ovarian cancer cells identifies FOXM1 overexpression in ovarian cancer. Mol Cancer Res 2012;10:914–24.
50. Iwasa T, Okamoto I, Takezawa K, Yamanaka K, Nakahara T, Kita A, et al. Marked anti-tumour activity of the combination of YM155, a novel survivin suppressant, and platinum-based drugs. Br J Cancer 2010;103: 36–42.